

Production of Antibiotic Nanoparticles Using Supercritical CO₂ as Antisolvent with Enhanced Mass Transfer

Pratibhash Chattopadhyay and Ram B. Gupta*

Department of Chemical Engineering, Auburn University, Auburn, Alabama 36839-5127

Drug delivery systems improve the therapeutic efficacy and safety of drugs by delivering them at a controlled rate depending on the body requirements and the site of action. These systems aid in reducing the amount of drug required, the number of doses, side effects, and bioinactivation. Currently, delivery systems for drug targeting and controlled release are being developed using drug nanoparticles. Several techniques, such as spray drying and milling, have been used in the past for the manufacture of drug nanoparticles, but these methods have several disadvantages. Supercritical fluid technologies such as RESS and SAS do provide novel methods for particle formation, but in most cases, they still cannot produce particles in the nanometer range (<300 nm) necessary for drug targeting and controlled release. In this work, we propose a technique that can produce drug particles in the nanometer range with a narrow size distribution. This new technique is a modification of the currently existing SAS technique and involves the use of a vibrating surface that atomizes the jet into microdroplets. The ultrasonic field generated by the vibrating surface also enhances mass transfer through increased mixing. The new technique is demonstrated for the production of tetracycline nanoparticles as small as 125 nm in size with a narrow size distribution. Particle sizes are easily controlled using this technique by changing the vibrational intensity of the vibrating surface.

Introduction

Nanoparticles are important in developing delivery systems for the controlled release of drugs. These systems can improve the drugs' therapeutic efficacy, in vitro and in vivo stability, bioavailability, targetability, and biodistribution to reduce toxicity.¹ The delivery systems involving nanoparticles studied so far include polymer nanoparticles with the drug dispersed within the polymer matrix, polymer nanoparticles with the drug adsorbed on the surface, drug nanoparticles coated with a biodegradable polymer, and nanoparticle suspensions for poorly soluble drugs.²

The oral form of immunization and drug delivery has obvious advantages over the parenteral form. Oral drug delivery is possible if absorption of the nanoparticle-sized drug carriers can be achieved in the gastrointestinal tract (GIT) in useful quantities. These carriers protect the labile drug molecules from degradation in the GIT and help in targeting therapeutic agents to the infected sites. The carrier systems act as a long-circulating drug reservoir from which drugs can be slowly released over a prolonged period. Antibiotics have been found to increase in efficacy or decrease in toxicity after being bound to nanoparticles. For example, the efficacy of ampicillin against both *Listeria monocytogenes* and *Salmella typhimurium* C5 was enhanced significantly when bound to polysohexyl nanoparticles, resulting in an improvement in the therapeutic index by 20-fold.^{3,4}

Apart from oral administration, nanoparticles can also be delivered parenterally through intravenous, subcutaneous, and intraperitoneal means. Nanoparticles have a higher dissolution rate, a higher saturation

solubility, and a greater adhesion when compared to microparticles.⁵ In addition, nanoparticles show increased rate of absorption in the GIT wall and a faster rate of diffusion into the blood stream, making them ideal for parenteral administration. Nanoparticles can also be used to increase the bioavailability of poorly soluble drugs when used as nanosuspensions. Nanosuspensions are dispersions of nanoparticles (5–1000 nm) in a fluid stabilized by using surfactants or, alternatively, by being adsorbed on polymers.⁵

Another major advantage of nanoparticles is that they are better at reaching the desired target organs when compared to larger particles. Jani and co-workers (1990),^{6,7} conducted experiments in which polystyrene spheres in the size range of 50 nm to 3 μ m were fed to rats. The extent of adsorption of 50-nm particles under the conditions of the experiment was 34%, and that of 100-nm particles was 25%, of which about 7% (50 nm) and 4% (100 nm) were in the liver, spleen, and bone marrow. Particles larger than 100 nm did not reach the bone marrow, and those larger than 300 nm were absent from the blood and were unable to penetrate heart and lung tissues.

Several methods have been used in the past for the manufacture of drug nanoparticles. Some of the conventional techniques include spray drying and ultrafine milling.^{8,9} The major disadvantage of these techniques is that they produce particles with a broad size distribution (0.5–25 μ m) and only a small fraction of particles in the nanometer range.¹⁰ Drug nanoparticles can also be prepared by a precipitation process, leading to the formation of hydrosols, but these methods have limitations because of the difficulties involved in containing and controlling particle growth. In recent years, however, supercritical fluid technologies such as rapid expansion of supercritical solutions (RESS)^{11–13} and supercritical antisolvent precipitation (SAS)^{14–16} have

* Author to whom correspondence should be addressed.
Phone: (334) 844-2013. Fax: (334) 844-2063. E-mail: gupta@auburn.edu.

emerged as attractive methods for drug and biological particle formation. Some of the advantages of these techniques include mild operating temperatures and the absence of residual solvent. The particles obtained by these techniques are 0.7–5.0 μm in size and have a narrow size distribution. Although these techniques are becoming increasingly popular, in most cases, they still do not produce particles predominantly in the nanometer range (<300 nm) necessary for drug targeting and controlled release. In the SAS process, the operating temperature, pressure, and concentration of the injecting solution have so far been investigated as size-control parameters, but none of these parameters have been found to produce a significant decrease in the particle size over a wide range. Again, extensive application of the RESS technique is limited by the solubility limit of the solid being precipitated in the supercritical fluid.

With this in mind, we proposed a technique that can be used to manufacture particles in the nanometer range having a very narrow size distribution. This new technique, supercritical antisolvent precipitation with enhanced mass transfer (SAS-EM),¹⁷ is a modification of the conventional SAS process and overcomes the currently existing limitations of the SAS process. Like the SAS process, SAS-EM also uses supercritical CO_2 as an antisolvent. The modification in the new technique is that it utilizes a surface vibrating at an ultrasonic frequency to atomize the solution jet into microdroplets. Moreover, the ultrasound field generated by the horn surface provides a velocity component in the y direction (direction normal to the vibrating surface) that greatly enhances turbulence and mixing within the supercritical phase and results in high mass transfer between the solution and the antisolvent. The combined effect of the fast rate of mixing between the antisolvent and the solution and the reduction of solution droplet size through atomization provides particles that are approximately 10 times smaller than those obtained from the conventional SAS process.

The use of high-energy sonic waves for particle precipitation using supercritical fluids has also been suggested by Subramaniam et al. (1997).¹⁸ In their case, a specialized nozzle of the type commercialized by Sonomist (model 600-1) was used to generate and focus the high-frequency sonic waves for atomization. A specialized nozzle was also employed by Randolph et al. (1993)¹⁹ in the precipitation of poly(L-lactic acid) particles using the SAS technique. The nozzle in their case was a Sonotek atomizer with a capillary tube, which was vibrated at 120 kHz to produce a narrow cylindrical spray. The proposed technique also uses high-frequency sound for atomization but the atomization process is brought about by introducing the solution on a vibrating surface in the form of a thin liquid film. No specialized nozzle has been used in this technique. Figure 1 and Table 1 illustrate the broad differences between the SAS-EM and SAS processes.

In this paper, we demonstrate the application of the SAS-EM technique to the formation of tetracycline nanoparticles required for pharmaceutical purposes. Tetracycline forms highly insoluble complexes with Ca(II) , Mg(II) , Fe(II) , and Al(III) ions, especially at neutral pHs in the presence of amino acids. This impedes their adsorption into the GIT when administered orally, resulting in a low bioavailability. In addition, the insolubility of the complexes leads to the deposition of significant amounts of tetracycline in the body, espe-

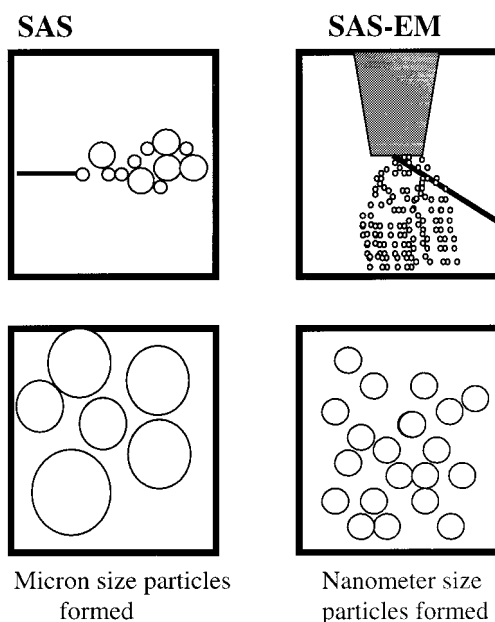


Figure 1. Broad differences between the SAS (left) and SAS-EM (right) techniques showing differences in the injection process and the size of particles formed.

cially on teeth and bones.²⁰ Nanoparticles of tetracycline can thus be used to solve this bioavailability problem and increase its safety. Different process parameters that can be used to control the particle size are also discussed in this paper.

Experimental Section

Materials. CO_2 and N_2 (both 99.9% pure, Airco), tetracycline (95% pure, lot no. 78H0745, Sigma), tetrahydrofuran (THF, 99.9% pure, Fisher Scientific), and KBr (99.9% pure, Aldrich) were used as received.

Apparatus. A schematic representation of the apparatus is shown in Figure 2. The main component of the apparatus consists of a high-pressure ultrasound precipitation cell (R) that is approximately 80 cm^3 in volume. A titanium horn (Sonics and Materials, Inc.) with a 1.25-cm-diameter tip is attached to the precipitation cell to provide the ultrasonic field and the vibrating surface necessary for atomization. The vibrations of the horn surface are generated by a 600-W (maximum power), 20-kHz ultrasonic processor (Ace Glass, Inc.). The ultrasonic processor is designed to deliver constant-amplitude vibrations. The amplitude of vibration of the ultrasonic horn is directly proportional to the total input power and can be controlled by adjusting the power supplied to the ultrasound transducer. A collection plate is placed inside the precipitation cell for collecting the particles. High pressure inside the cell is generated using a HIP hand pump (C). Valves V1 and V2 are used to fill the HIP hand pump with fresh CO_2 . The temperature inside the precipitation cell is maintained by placing it in a constant-temperature water bath. The solution containing the solid to be precipitated is injected inside the precipitation cell using a "solution injection device" (S), which consists of a stainless steel cylinder containing a piston. The piston divides the cylinder into two chambers. The antibiotic solution is placed inside one of these chambers and is delivered into the cell by using pressurized nitrogen in the other chamber. The device S is connected to the precipitation cell by means of a 75- μm -i.d. fused-quartz capillary tube.

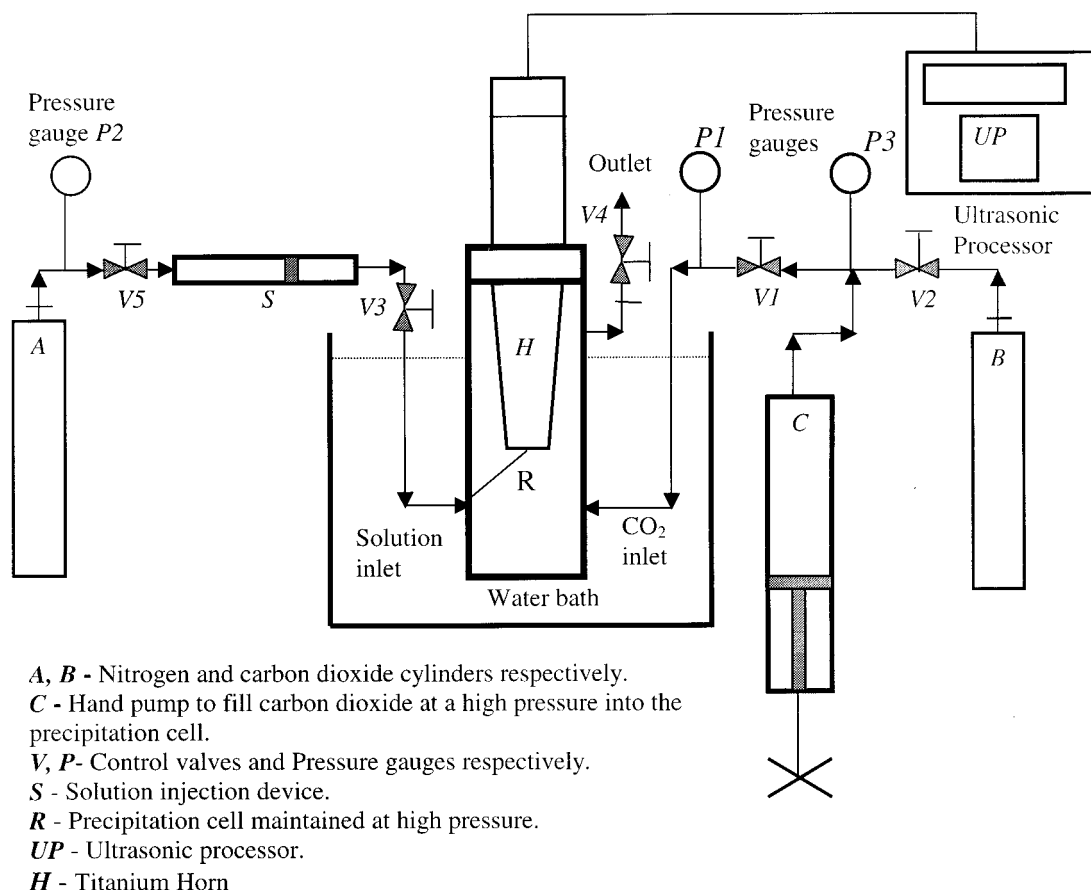


Figure 2. Schematic diagram of the SAS-EM apparatus.

Table 1. Differences between the Conventional SAS Technique and the New SAS-EM Technique

SAS Technique	SAS-EM Technique
Droplet Formation	
Droplet formation is due to jet break up of the solution jet that is injected into the supercritical fluid phase medium.	Droplet formation is due to atomization of the jet into microdroplets caused by the vibrating horn surface at an ultrasonic frequency of 20 kHz.
Mass Transfer Rate	
Depends on the solvent in use and is the rate of transfer of the solvent between the droplet and the supercritical fluid medium.	Also depends on the solvent in use, but there is an enhanced rate of mass transfer between the droplet and the supercritical fluid due to increased mixing and turbulence caused by the ultrasonic field.
Droplet/Particle Motion	
Droplet/particle motion within the supercritical fluid phase is due to the momentum imparted by the solution jet velocity.	Droplet/particle motion within the supercritical fluid phase is due to the vibrating ultrasonic surface, which propels the droplets and particles away from the horn at a rapid rate.
Particle Sizes Obtained	
Sizes of the particles obtained are fairly small, in the micrometer range (1–5 μm).	Sizes of the particles obtained by this method are much smaller, in the nanometer range (100–500 nm).
Particle Size Adjustability	
Particles sizes can be slightly controlled by changing the density of the supercritical fluid, by varying the pressure and the temperature of the supercritical fluid.	Particle sizes can be controlled to a great extent by changing the power supplied to the vibrating surface (i.e., changing the amplitude of the vibrating surface). In addition, minor control can also be obtained by changing the supercritical fluid density.

A pressure drop of 28 bar is maintained across the capillary tube and the device S in order to spray the solution inside the precipitation cell. A capillary tube is placed at an angle of 40° with respect to the horn surface so that the capillary opening just touches the horn surface. Supercritical CO_2 is fed into the precipitation cell through the inlet port located at the bottom of the vessel. Valve V1 is used to control the flow of supercritical CO_2 into the high-pressure cell. The pressure inside the cell is measured using pressure gauge P1. The outlet port is located on top of the precipitation cell, and valve V4 is used to control the depressurization

process. The pressure difference across the capillary and the solution injection device is measured using pressure gauges P2 and P1.

Procedure. All of the precipitation experiments were carried out in the batch mode and in an identical manner. First, the ultrasonic precipitation cell was filled with carbon dioxide to the desired operating pressure. The temperature inside the cell was maintained using a water bath. Approximately 1.5–2.0 g of THF containing tetracycline (5 mg/mL) was then loaded into the solution injection device (S). The ultrasonic horn inside the cell was then switched on at the desired vibration

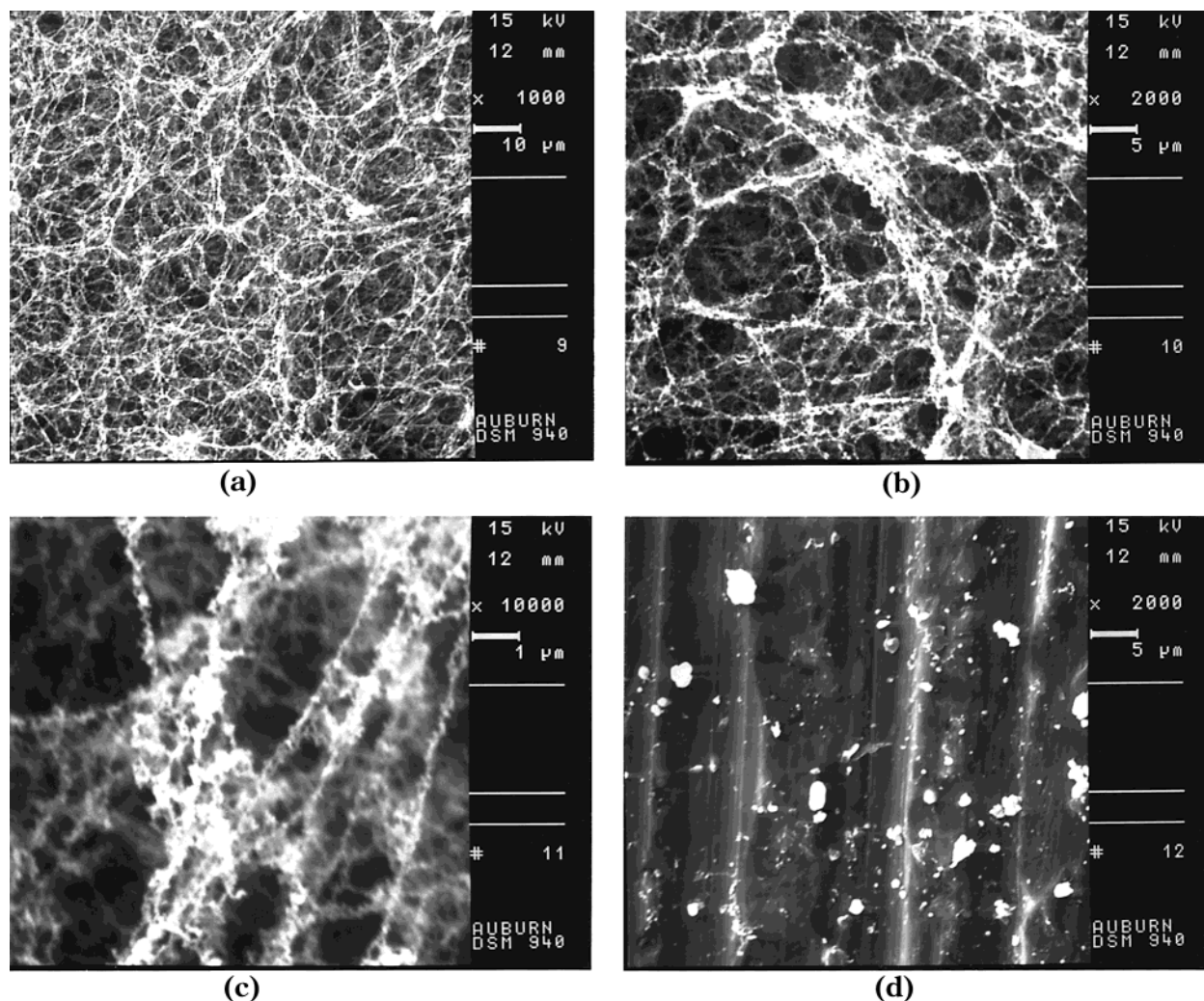


Figure 3. SEM images of tetracycline fibers and particles produced by the SAS-EM process at 96.5 bar pressure and 35 °C with no ultrasound. Most of the solid is in the form of fibers, as shown in parts a–c. A few particles were also obtained, as shown in part d.

amplitude by adjusting the input power, and the solution was introduced into the precipitation cell through the 75- μm capillary tube placed against the horn surface at an angle of 40°. As soon as the solution jet was introduced into the cell, it was atomized by the horn surface into tiny droplets, and particles were formed as a result of the rapid removal of the solvent by supercritical CO_2 from these droplets. The motion between the particles inside the cell was increased by the ultrasonic field generated by the horn surface, which prevented agglomeration. The injection process was typically completed in 2–3 min, and the power supply to the ultrasonic horn was turned off thereafter.

Next was the washing step in which residual THF still dissolved in supercritical CO_2 was removed by continuously purging the precipitation cell with fresh CO_2 . The complete cleaning process required approximately 7–8 times the vessel (R) volume of fresh CO_2 . The precipitation cell was then allowed to slowly depressurize until it reached ambient pressure. The cell was then opened and the collection plate was removed and taken for particle analysis.

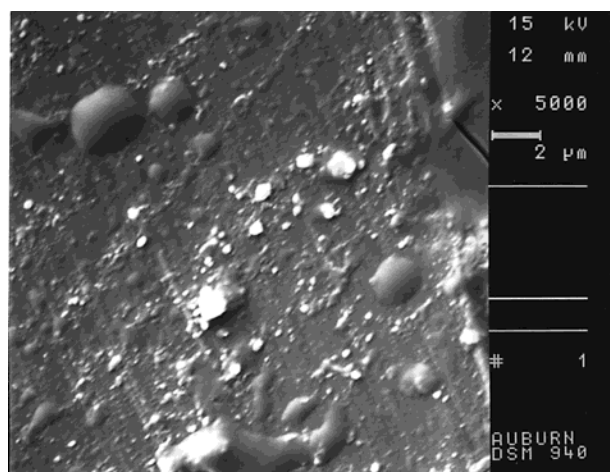
Analysis and Characterization. *Measurement of Particle Size and Distribution.* Size analysis was carried out using a scanning electron microscope (Zeiss, model DSM940). For analysis portions of the collection plate containing the particles were cut carefully, placed onto an aluminum stub, and then coated with gold/palladium

using a sputter coater (Pelco, model Sc-7). SEM micrographs of the particles on different regions of the collection plate were then obtained. From the SEM micrographs, the volume particle size distribution and the number-average size and standard deviation of the particles were determined by measuring the diameters of 100–200 randomly selected particles from each experiment. Care was taken to ensure that each SEM micrograph represented an overall distribution of all the obtained particles.

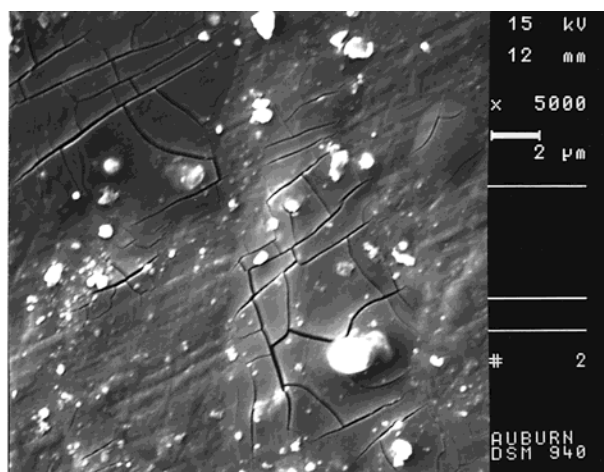
FTIR Analysis. The FTIR spectrum was recorded using a Perkin-Elmer Spectrum 2000 spectrophotometer in the range of 800–4000 cm^{-1} . Tetracyclines are not sufficiently soluble in convenient solvents such as chloroform, and hence their IR spectra are usually determined using KBr wafers or disks. The tetracycline sample was mixed with KBr, dried at 100 °C for 60 min, and pressed to obtain the self-supporting disks. These disks were then placed inside the infrared spectrophotometer to record the spectrum.

Results

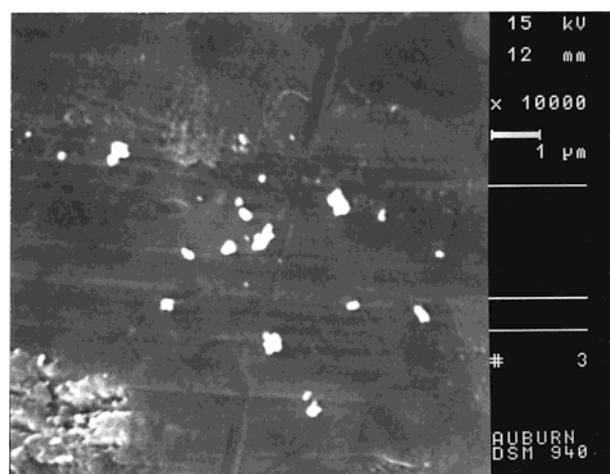
The solution jet atomization and mixing within supercritical media are closely related to the degree of vibration of the horn surface. Experiments were conducted to examine the effect of changes in the amplitude of vibration of the horn surface on the size of the



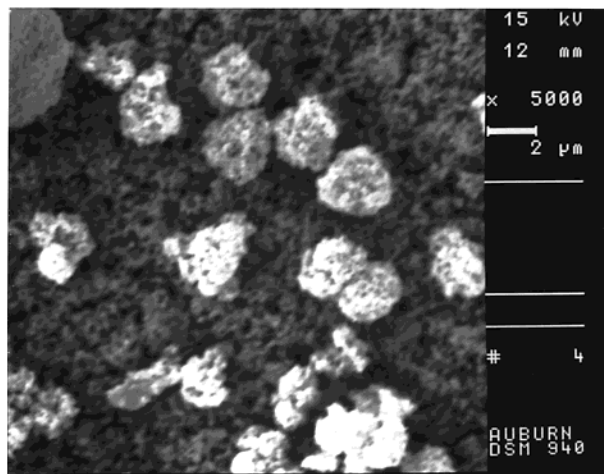
(a1)



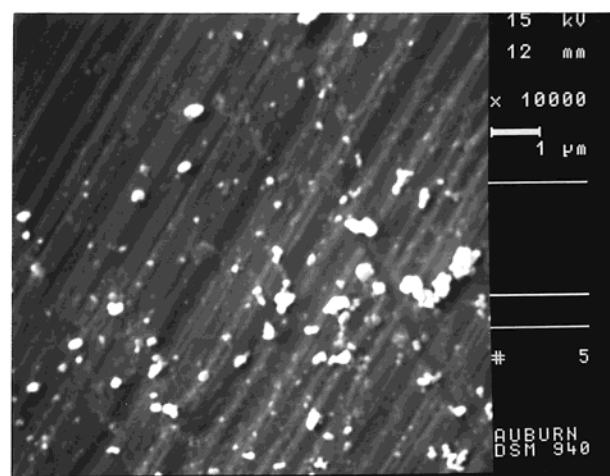
(a2)



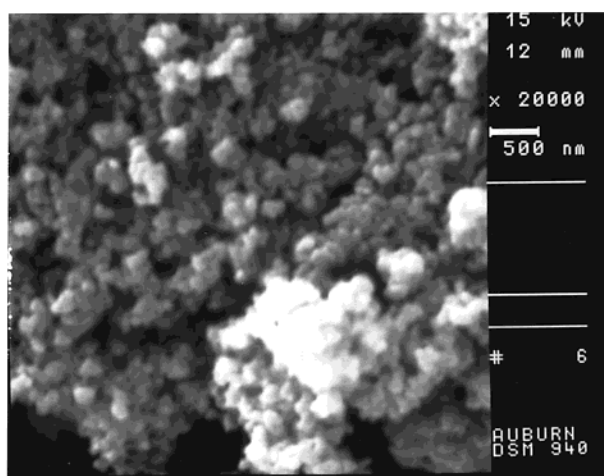
(b1)



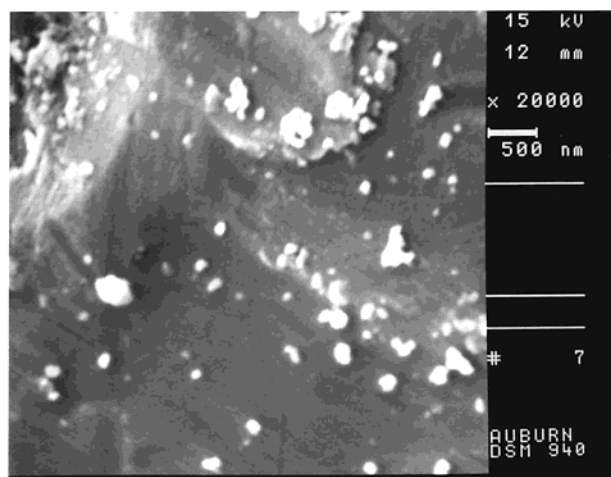
(b2)



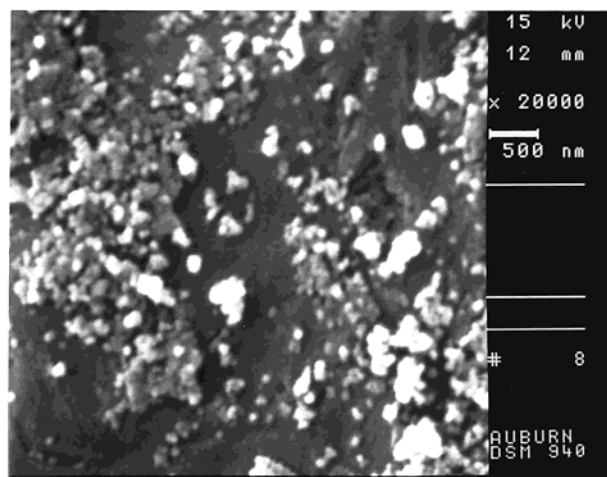
(c1)



(c2)



(d1)

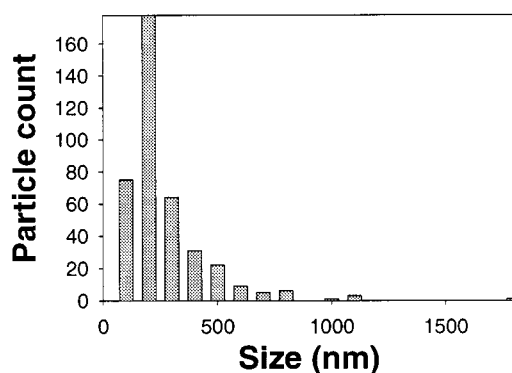


(d2)

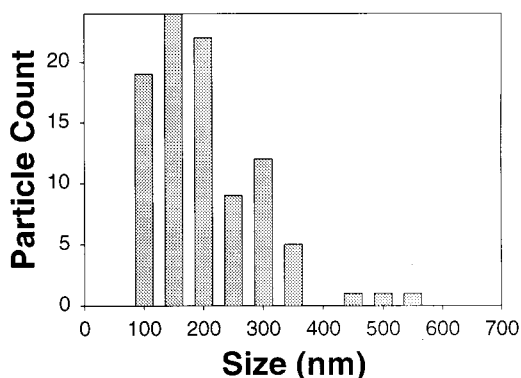
Figure 4. SEM images of tetracycline particles produced by the SAS-EM process at 96.5 bar, 35 °C, and (a1, a2) 30 W, (b1, b2) 60 W, (c1, c2) 90 W, and (d1, d2) 120 W of supplied power. The mean size of the particles obtained in each case is (a1, a2) 400 nm, (b1, b2) 230 nm, (c1, c2) 200 nm, and (d1, d2) 125 nm.

tetracycline particles formed. The precipitation cell was kept constant at 96.5 bar and 35 °C while the frequency of the titanium horn was maintained at 20 kHz. The solution jet was then introduced into the cell at different horn amplitudes corresponding to 0–20% of the total power supplied. With no ultrasound and when the ultrasound horn amplitude was zero tetracycline fibers around 2 μm in diameter were obtained. A few particles having a mean size of 800 nm were also obtained, but most of the solid was in the form of a fine mesh of fibers having a low mechanical strength, as shown in Figure

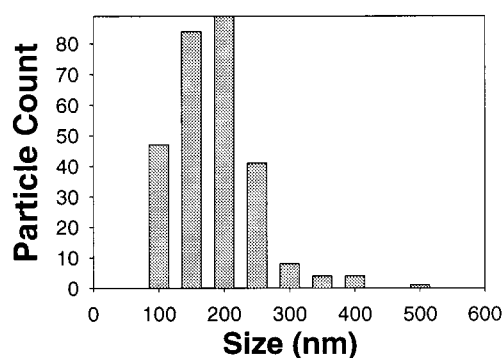
3a–d. It is important to note here that the experiment conducted at zero amplitude was similar to conventional SAS. The nozzle in this case was placed parallel to the horn surface without touching the horn. Our SAS experiments produced particles that were similar to those obtained by others for similar compounds.^{10,11} As the power supply to the horn was increased and as the horn was made to vibrate with larger amplitude, there was a considerable decrease in the size of the particles obtained, as shown in Table 1. Figure 4a1–d2 presents SEM micrographs of particles obtained from experi-



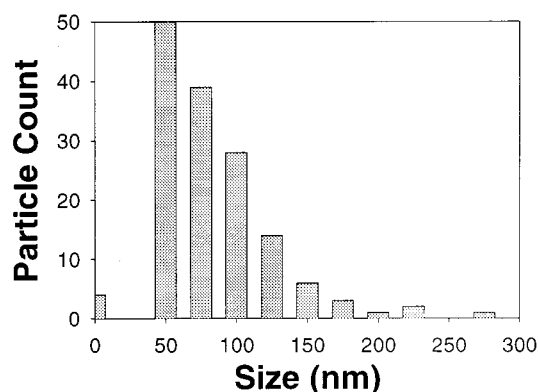
(a) at 30 W power supply.



(b) at 60 W power supply.



(c) at 90 W power supply.



(d) at 120 W power supply.

Figure 5. Size distribution of tetracycline particles obtained from experiments conducted at varying ultrasound powers.

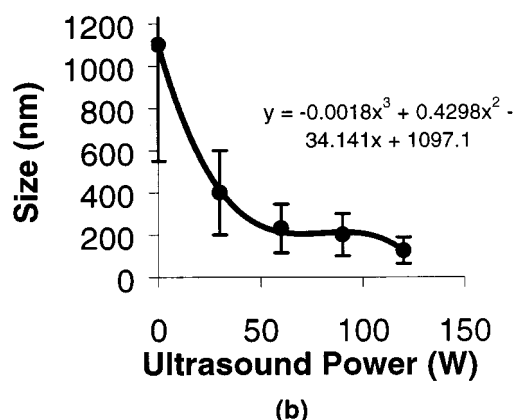
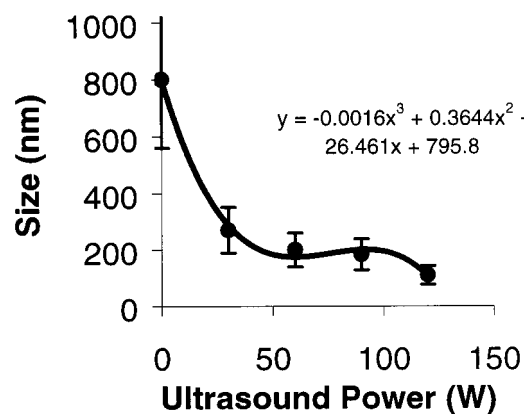


Figure 6. Average tetracycline particle size versus power supply to the horn: (a) number-average and (b) volume-average.

Table 2. Results of the Experiments Conducted at Different Ultrasound Powers at 96.5 bar and 37 °C

power supplied (W)	particle size number-average (nm)	particle size volume-average (nm)	standard deviation (nm)
0	800	1100	970
30	270	400	480
60	200	230	172
90	184	200	133
120	110	125	75

ments conducted at the different horn amplitudes. Figure 5a–d shows a comparison of particle size distribution of tetracycline particles obtained from experiments conducted at different ultrasound horn amplitudes.

Vibration Intensity (Ultrasound Power Supply) as the Size Control Parameter. From the results in Table 2, it is interesting to note that, with an increase in the power supply (i.e., in the ultrasound horn amplitude), there is a considerable decrease in the particle size. Particles as small as 125 nm in size are obtained when the power supply is 120 W. Figure 6, showing the relationship between the average particle size and the power supplied to the horn, clearly illustrates this trend. The volume-average (S_{vol}) and number-average (S_{num}) particle sizes are related to the ultrasound power (P) by

$$S_{vol} = -0.0016P^3 + 0.3644P^2 - 26.461P + 795.8 \quad (1)$$

$$S_{num} = -0.0018P^3 + 0.4298P^2 - 34.141P + 1097.1 \quad (2)$$

where S_{vol} and S_{num} are in nanometers and P is in watts.

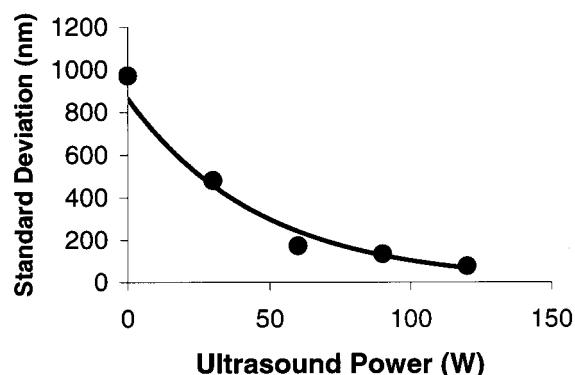


Figure 7. Standard deviation in the size of the tetracycline particles versus power supplied to the ultrasound horn.

In addition to the decrease in the particle size, there is also a considerable decrease in the standard deviation in the particle size at higher horn vibration amplitudes, as shown in Figure 7. This is due to the narrow droplet size distribution obtained by the SAS-EM technique, which leads to the formation of more uniform sized particles. Bindal et al. (1985),²¹ in their study of the droplet size distribution as a function of amplitude for atomizers with liquid flowing through a channel within the ultrasonic horn observed that there is an increase in the droplet size with increasing amplitude. The effect was attributed to cavitation in the liquid flowing through the channel that occurred even before it came out onto the surface. In SAS-EM, because of the high operating pressure of 96.5 bar and the fact that the liquid hits against the horn surface as opposed to traveling through a channel in the horn, cavitation cannot take place.

Effect of Ultrasound in the Precipitation Process. Once the tetracycline solution is introduced into supercritical CO₂ and onto the horn surface, the liquid spreads evenly over the surface, forming a thin liquid film. Because the horn surface is vibrating ultrasonically (at a frequency of 20 kHz) normal to the liquid film, a set of wavelets forms on the free liquid surface. The oscillatory vibrations of the liquid surface cause the wavelets to increase in amplitude until the tips break off and droplets are emitted from the surface into the supercritical fluid media.²²

The droplet diameter is proportional to the wavelength of the liquid film surface and can be determined via²³

$$D = 0.34 \left(\frac{8\pi\sigma}{\rho F^2} \right)^{1/3} \quad (3)$$

where σ is the surface tension, ρ is the density of the liquid, and F is the vibration frequency.

Once the droplets are present inside the supercritical fluid, rapid transfer of CO₂ into these droplets and of THF out of these droplets causes the droplets to expand rapidly. This subsequently decreases the droplets' ability to keep tetracycline dissolved, causing the tetracycline to precipitate out as fine particles. The precipitation starts at the supercritical fluid–liquid interface and then propagates inside the liquid, thus attracting the solute toward the interface^{24,25} and causing the formation of porous, spherical balloon-like structures made up of tiny particles loosely coalesced together. Similar structures, around 20 μ m in diameter, were observed by Reverchon et al. (1998)²⁴ during the SAS precipita-

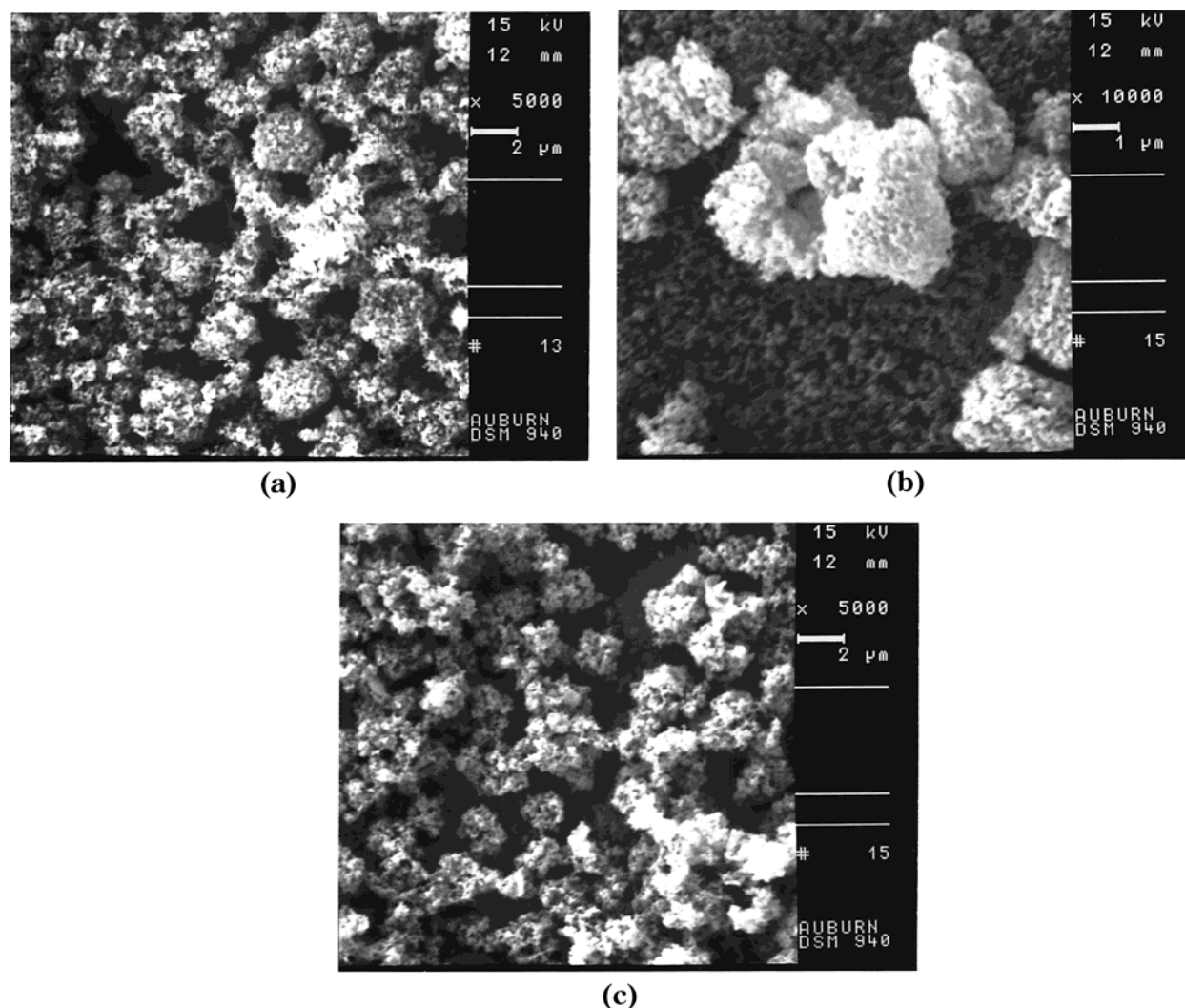


Figure 8. SEM images of tetracycline particles produced by the SAS-EM process at 96.5 bar, 35 °C, and (a, b) 60 and (c) 90 W of supplied power. In this case, the tetracycline particles are agglomerated together as spherical balloons of size 2–5 μm.

tion of AcY particles from dimethyl sulfoxide solvent. In our case, we observed similar spherical structures for experiments conducted at 96.5 bar, 37 °C, and an ultrasound horn amplitude of 10% of the total power. The sizes of these structures are much smaller and range between 1 and 5 μm, as shown in Figure 8. The decrease in size could be due to a smaller initial droplet diameter and narrower droplet size distribution produced by the SAS-EM technique when compared to the conventional SAS technique.

Another important factor that determines the antibiotic particle size is the mass transfer rate of the supercritical fluid into the liquid droplet. Rapid mass transfer between supercritical CO₂ and THF causes the tetracycline particles to precipitate out as tiny nuclei, which, in turn, coalesce to form larger particles. Better mixing characteristics can thus affect the particle size by enhancing the mass transfer rates between the solution and the supercritical phase and also by preventing the particles from agglomerating.²⁶ Several researchers^{27–29} have demonstrated that ultrasonic standing waves at appropriate intensities can cause increased particle motion through the nonuniform distribution of pressure and velocity components in a standing ultrasonic wave field. This same phenomenon is observed in the SAS-EM technique. The ultrasound field provides a velocity component in the *y* direction

(direction normal to the vibrating surface), which greatly enhances the turbulence within the supercritical phase and results in a high mass transfer rate because of the increased mixing. Increased mixing also prevents the agglomeration of particles. In the SAS-EM technique, the combined effects of jet atomization into very tiny droplets and high rates of mass transfer through increased mixing within the supercritical phase cause the particle sizes to be extremely small.

Effects of Ultrasound on the Precipitated Particles. *Ultrasonic Streaming.* Once tetracycline particles have been precipitated inside the chamber, the particles experience different types of steady flows in the presence of the ultrasonic field, leading to a phenomenon known as ultrasonic streaming.³⁰ These flows exist both in the ultrasonic free field and the also near the obstacles and are responsible for the constant motion of the particles inside the chamber that prevents them from agglomerating together. The velocity of these streams can be approximated as³¹

$$\rho_0 v_0^2(x)/2 = w(0) - w(x)$$

where v_0 is the flow velocity, ρ is the fluid density, and w is the acoustic energy density. In essence, the above equation is the law of conservation of energy where the left side represents the kinetic energy per unit volume

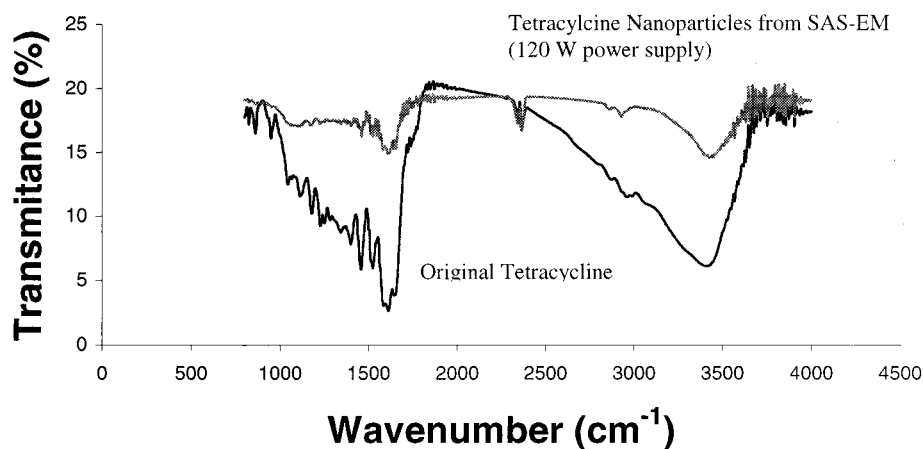


Figure 9. IR spectra of tetracycline as obtained from the manufacturer and after processing using the SAS-EM technique.

of the medium and the right side is the difference between the average acoustic densities at the ultrasonic source and at a distance x from the source.³¹

Inside the precipitation chamber the flow of liquid is away from the ultrasonic radiator and is accompanied by inflow from regions where the liquid encounters a solid obstacle. As a result, continuous stationary circulating currents are generated, which keep the particles in constant motion. Depending on the ultrasonic intensity and the size of the vessel, the currents can be laminar or turbulent. At high ultrasonic intensities, the acoustic flow becomes extremely turbulent and gives rise to intense mixing of particles within the supercritical fluid, greatly enhancing the rate of mass transfer between the solvent and the supercritical medium and leading to the precipitation of small particles.

Ultrasonic Forces on the Particles. Apart from the motion of tetracycline particles resulting from ultrasonic streaming, forces such as gravitational, mechanical, acoustic–radiation–pressure, and hydrodynamic forces are also experienced by the particles because of the ultrasonic field. Suspended tetracycline particles can be considered neutrally buoyant, and hence, gravitational effects, although present, can be neglected. The particles experience mechanical forces when they encounter the vibrating surface of the horn. These forces can break the larger particles into smaller sizes or propel them away from the horn surface causing them to move around in the supercritical phase.

The particles experience an acoustic radiation pressure that can be defined as the difference between the average pressure at a surface moving with the displacement due to the sound and the pressure that would have existed in a fluid of the same mean density at rest.³²

The tetracycline particles suspended in the ultrasonic field also experience different hydrodynamic forces, such as Bjerknes forces³³ and Bernoulli's forces.³⁴ Bjerknes forces acting between the particles can be attractive or repulsive depending on the value of the phase difference between the particle velocities. Bernoulli's forces can lead to the coagulation of particles in high-frequency ultrasonic fields.³⁴

FTIR Analysis of Tetracycline Nanoparticles. A FTIR analysis was performed to determine whether there is any difference in the structures of the original tetracycline (as supplied by the manufacturer) and that obtained from the precipitation experiments using the SAS-EM technique with 120 W of supplied power. Figure 9 shows the IR spectra obtained in the two cases.

A comparison of the two spectra shows that there is no variation in the molecular structure of the two tetracyclines. In the case of tetracycline, the carbonyl region between 1500 and 1600 cm^{-1} and the amide region between 3000 and 4000 cm^{-1} are of greatest importance to medicinal chemists. These regions seem to be similar for both the original and the SAS-EM-precipitated tetracycline samples, confirming that no structural changes took place in the SAS-EM process.

Conclusions

We have successfully prepared tetracycline nanoparticles as small as 125 nm in size using the SAS-EM technique. The particles obtained by this process are up to 8 times smaller than those obtained from the conventional SAS process. Particle sizes in the SAS-EM technique can easily be controlled by adjusting the power supplied to the transducer. At higher ultrasound powers, in addition to a decrease in the particle size, the standard deviation in the particle size is also much smaller. Thus, particles having a narrower size distribution are obtained. FTIR analysis of the tetracycline nanoparticles shows that there is no change in the molecular structure of tetracycline as a result of exposure to ultrasound.

Acknowledgment

Financial support from the NSF (CTS-9801067) and the NIH (James A. Shannon Director's award to R.B.G., 1R55RR13398-01) is appreciated. The authors are also thankful to Dr. Lalit Chordia of Thar Designs, Inc. (www.thardesigns.com) for technical discussions.

Literature Cited

- (1) Labhasetwar, V. Nanoparticles for drug delivery. *Pharm. News* **1997**, 4 (6), 28.
- (2) Langer, R. New Methods of Drug Delivery. *Science* **1990**, 249, 1527.
- (3) Fattal, E.; Youssef, M.; Couvreur, P.; Andremont, A. Treatment of experimental salmonellitis in mice with ampicillin-bound nanoparticles. *Antimicrob. Agents Chemother.* **1989**, 33, 1540.
- (4) Fourage, M.; Dewulf, M.; Couvreur, P.; Roland, M.; Vranckx, H. Development of dehydroemetine nanoparticles for the treatment of visceral leishmaniasis. *J. Microencapsulation* **1989**, 5, 29.
- (5) Diederich, J. E.; Muller, R. H. *Future Strategies for Drug Delivery with Particulate Systems*; Medpharm Scientific Publishers: Berlin, 1998.

- (6) Jani, P.; Halbert, G. W.; Langridge, J.; Florence, A. T. Nanoparticle Uptake by the Rat Gastrointestinal Mucosa: Quantitation and Particle Size Dependency. *J. Pharm. Pharmacol.* **1990**, *42*, 821.
- (7) Jani, P.; Halbert, G. W.; Langridge, J.; Florence, A. T. The uptake and translocation of latex nanospheres and microspheres after oral administration in rats. *J. Pharm. Pharmacol.* **1989**, *41*, 809.
- (8) Nass, R. Pharmaceutical Suspensions. In *Pharmaceutical Dosage Forms*; Lieberman, H. A., Rieger, M., Banker, B., Eds.; Marcel Dekker: New York, 1988.
- (9) Hixon, L.; Prior, M.; Prem, H.; Van Cleef, J. Sizing materials by crushing and grinding. *Chem. Eng.* **1990**, *97*, 99.
- (10) Reverchon, E.; Della Porta, G. Production of antibiotic micro- and nanoparticles by supercritical antisolvent precipitation. *Powder Technol.* **1999**, *106*, 23.
- (11) Reverchon, E.; Della Porta, G.; Trolino, A. D.; Pallado, P.; Stassi, A. Micronization of Griseofulvin in Supercritical CHF₃. *Ind. Eng. Chem. Res.* **1995**, *34* (11), 4087.
- (12) Helfgen, B.; Hils, P.; Holzknicht, C.; Turk, M.; Schaber, K. Simulation of particle formation during the rapid expansion of supercritical solutions. *J. Aerosol Sci.* **2001**, *32* (3), 295.
- (13) Charoentachitrakool, M.; Dehghani, F.; Foster, N. R.; Chan, H. K. Micronization by Rapid Expansion of Supercritical Solutions to Enhance the Dissolution Rates of Poorly Water-Soluble Pharmaceuticals. *Ind. Eng. Chem. Res.* **2000**, *39* (12), 4794.
- (14) Winters, M. A.; Knutson, B. L.; Debenedetti, P. G.; Sparks, H. G.; Przybcien, T. M.; Stevenson, C. L.; Prestrelski, J. S. Precipitation of Proteins in Supercritical Carbon Dioxide. *J. Pharm. Sci.* **1996**, *85*, 586.
- (15) Yeo, S.-F.; Lim, G.-B.; Debenedetti, P. G.; Bernstein, H. Formation of Microparticulate Protein Powders Using a Supercritical Fluid Antisolvent. *Biotechnol. Bioeng.* **1993**, *41*, 341.
- (16) Reverchon E. Supercritical antisolvent precipitation of micro- and nanoparticles. *J. Supercrit. Fluids* **1999**, *15*, 1.
- (17) Gupta, R. B.; Chattopadhyay, P. Method of Forming Nanoparticles and Microparticles of Controllable Size Using Supercritical Fluids and Ultrasound. U.S. Provisional Patent 60/206,644, 2000.
- (18) Subramaniam, B.; Saim, S.; Rajewski, R. A.; Stella, V. Method for Particle Precipitation and Coating Using Near-Critical and Supercritical Antisolvents. U.S. Patent 5,833,891, 1997.
- (19) Randolph, T. W.; Randolph, A. D.; Mebes, M.; Yeung, S. Sub-Micrometer-Sized Biodegradable Particles of Poly(L-lactic acid) via the GAS Antisolvent Spray Precipitation Process. *Biotechnol. Prog.* **1993**, *9*, 429.
- (20) Mitscher, L. A. *The Chemistry of Tetracycline Antibiotics*; Medicinal Research Series; Marcel Dekker: New York, 1978; Vol. 9.
- (21) Bindal V. N.; Jain, S. K.; Kumar, Y. Performance Characteristics of an Ultrasonic Atomizer. *Indian J. Technol.* **1986**, *24*, 153.
- (22) Lang, R. J. Ultrasonic atomization of liquids. *J. Acoust. Soc. Am.* **1962**, *34*, 6.
- (23) Topp, M. N. Ultrasonic Atomization—A Photographic study of the Mechanism of Disintegration. *Aerosol Sci.* **1973**, *17*.
- (24) Reverchon, E.; Della Porta, G.; Trolino, A. D.; Pace, S. Supercritical Antisolvent Precipitation of Nanoparticles of Superconductor Precursors. *Ind. Eng. Chem. Res.* **1998**, *37*, 952.
- (25) Bertuccio, A.; Vaccaro, F.; Pallado, P. Drug encapsulation using compressed gas antisolvent precipitation. Presented at the 4th Italian Conference on Supercritical Fluids and Their Applications, Capri, Italy, Sept 7–10, 1997.
- (26) Palakodaty, S.; York, P. Phase Behavioral Effects on Particle Formation Process Using Supercritical Fluids. *Pharm. Res.* **1999**, *16*, 976.
- (27) Mandralis, Z. I.; Fekke, D. L. Fractionation of Suspensions Using Synchronized Ultrasonic and Flow Fields. *AIChE J.* **1993**, *39*, 197.
- (28) Apfel, R. E. Radiation Pressure—Principles and Application to Separation Science. *Fortschr. Acustik DAGA* **1990**, *19*.
- (29) Schram, C. J. Manipulation of Particles, U.S. Patent No. 4,743,351, 1988.
- (30) Abramov O. V. *High-Intensity Ultrasonics: Theory and Industrial Applications*; Gordon and Breach Science Publishers: Amsterdam, 1998.
- (31) Shutilov V. A. *Fundamental Physics of Ultrasound*; Gordon and Breach Science Publishers: Amsterdam, 1988.
- (32) Rayleigh, B.; Strutt, J. W. *Theory of Sound*; Macmillan and Co.: New York, 1896.
- (33) Lamb, H. *Hydrodynamics*; Dover Publications: New York, 1945.
- (34) Mednikov, E. P. *Acoustic Coagulation and Precipitation of Aerosols*; Translation from the Russian by Larrick, C. V.; Consultants Bureau: New York, 1965.

Received for review January 10, 2001

Revised manuscript received May 16, 2001

Accepted May 16, 2001

IE010040R